Computers and Electronics in Agriculture 124 (2016) 23–28

Contents lists available at ScienceDirect

Computers and Electronics in Agriculture

journal homepage: www.elsevier.com/locate/compag

Stress wave velocity patterns in the longitudinal–radial plane of trees for defect diagnosis

Guanghui Li [a,b,*], Xiang Weng [c], Xiaocheng Du [c], Xiping Wang [d], Hailin Feng [c]

[a] School of Internet of Things (IoT) Engineering, Jiangnan University, Wuxi, China
[b] Engineering Research Center of IoT Technology Applications (Ministry of Education), Jiangnan University, Wuxi, China
[c] School of Information Engineering, Zhejiang A&F University, Hangzhou, China
[d] USDA Forest Service, Forest Products Laboratory, Madison, WI, USA

ARTICLE INFO

Article history:
Received 29 October 2015
Received in revised form 22 March 2016
Accepted 25 March 2016

Keywords:
Defect
Inspection
Nondestructive testing
Stress wave velocity
Urban trees

ABSTRACT

Acoustic tomography for urban tree inspection typically uses stress wave data to reconstruct tomographic images for the trunk cross section using interpolation algorithm. This traditional technique does not take into account the stress wave velocity patterns along tree height. In this study, we proposed an analytical model for the wave velocity in the longitudinal–radial (*LR*) plane of a live tree. Both field and laboratory stress wave testing were conducted to determine the stress wave velocity patterns in healthy and defective trees. The results showed that the ratio of the wave velocity at a propagation path angle θ (with respect to the radial direction) to the radial velocity in healthy trees approximated a second-order parabolic curve with respect to the symmetric axis ($\theta = 0$). Our analysis of the velocity patterns indicated that the measured velocities in healthy trees were in a good agreement with the theoretical models. The results of this preliminary study indicated that the stress wave velocity patterns can be used to diagnosis internal defects in urban trees and improve the accuracy of 3D tomographic images in tree inspection applications.

1. Introduction

Effective nondestructive testing methods capable of locating and quantifying wood decay and defects are needed by urban forest managers and arborists to determine the physical condition of trees and promote public safety. As a simple and low-cost nondestructive testing technique, stress wave method has been commonly used to assess internal conditions of wood structural members in buildings, timber bridges, and other timber structures (Pellerin and Ross, 2002; Ross and Pellerin, 1994). Stress wave velocity measured in trees has also been found effective in detecting moderate to severe decay in urban trees (Lawday and Hodeges, 2000; Wang et al., 2004; Wang, 2013; Hasegawa et al., 2012; Najafi et al., 2009; Guntekin et al., 2013). More recent development of efficient inversion algorithms enables stress wave techniques to be applied to urban trees to construct two dimensional (2D) acoustic tomograms for better revealing the internal condition of a tree trunk (Berndt et al., 1999; Bucur, 2003; Divos and Divos, 2005; Lin et al., 2008; Socco et al., 2004). Some commercial acoustic equipment such as Picus Sonic Tomograph (Argus Electronic Gmbh, Rostock, Germany), ArborSonic 3D Acoustic Tomograph (Fakopp Enterprise, Agfalva, Hungary), and Arbotom (RinnTech, Heidelberg, Germany) are now available for inspectors to obtain a 2D tomogram image by testing a tree's cross-section or 3D tomogram images through testing multiple cross-sections in a tree trunk.

However, the interpretation of an acoustic tomogram is not straight forward. A better understanding of wave velocity patterns in trees is critical to developing reliable and effective imaging software for internal decay detection. Dikrallah et al. (2006) presented an experimental analysis of acoustic anisotropy of wood, in particular the dependence of propagation velocities of stress waves on natural anisotropy axis in the cross section. They reported a significant difference in wave velocity between the waves propagating through the whole volume and the waves guided on bars. Maurer et al. (2005) studied the anisotropy effects on time-of-flight based tomography assuming an elliptic anisotropy where the angle dependent velocity v can be written as $v = v_{radial}\,(1 - \varepsilon \sin(\phi - \varphi)^2)$, where ϕ is the ray angle, φ represents the azimuth of the v_{radial} direction relative to the axis of the coordinate system, and ε specifies the degree of anisotropy. Liang et al. (2010) showed that stress waves traveled fastest in radial direction and that velocity decreased as the wave propagation path

* Corresponding author at: School of Internet of Things (IoT) Engineering, Jiangnan University, Wuxi, China.
E-mail address: ghli@jiangnan.edu.cn (G. Li).

http://dx.doi.org/10.1016/j.compag.2016.03.021
0168-1699/

shifted toward to tangential direction. Velocity also increased as the number of annual rings increased. Li et al. (2014) studied stress wave velocity patterns in black cherry trees and found that the ratio of tangential velocity to radial velocity in sound healthy trees approximated a second-order parabolic curve with respect to the symmetric axis $\theta = 0$ (θ is the angle between wave propagation path and radial direction). The analytical model was found in excellent agreement with the real data from healthy trees. Socco et al. (2004) also pointed out that the marked anisotropy of longitudinal direction properties could create numerous difficulties in constructing 3D tomographic images for trees. They considered longitudinal velocity a "less diagnostic" parameter for decay detection than the corresponding tangential and radial velocity. In investigating the effect of grain angle on longitudinal stress wave velocity in lumber, Gerhards (1982) found that grain angle had a greater effect on speed: over 1 percent loss per degree increase in grain angle up to about 30°. The effect of grain angle on MOE and tensile strength can be approximated by the Hankinson-type formula (USDA Forest Products Laboratory, 2010).

The objectives of this study were to investigate the stress wave velocity patterns in the *LR* plane of live trees and examine the effect of internal tree defect on the velocity pattern. We proposed a theoretical model of longitudinal wave velocity in *LR* plane of sound live trees and demonstrated the effectiveness of the theoretical model as a tool for tree defect diagnosis.

2. Theoretical analysis of stress wave velocity pattern in *LR* plane of live trees

Fig. 1 shows the coordinate system of an ideal tree trunk. Here, *L* represents the longitudinal or fiber direction, *R* represents the radial direction, and *T* is the tangential direction. For a longitudinal stress wave testing of wood, assume that ***OS*** is the stress wave propagation path in the *LR* plane, ***O*** is the first sensor for collecting the start stress wave signal, and ***S*** is the second sensor for sensing the propagating wave signal. In addition, α is the angle between the wave propagation path and the fiber direction, and θ is the angle between radial direction and the wave propagation path. So, $\alpha + \theta = 90°$.

Hankinson's formula provides a mathematical relationship that can be used to predict the off-axis uniaxial compressive strength of wood. The formula can also be used to compute the fiber stress or the stress wave velocity as a function of grain angle in wood (Li et al., 2014). The stress wave velocity at grain angle α can be obtained from the Hankinson formula:

$$V(\alpha) = \frac{V_l V_r}{V_l \sin^2 \alpha + V_r \cos^2 \alpha} \tag{1}$$

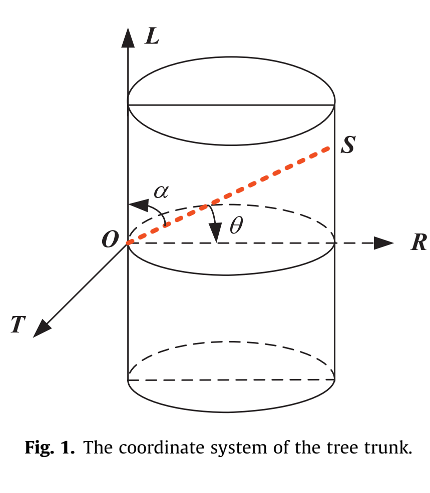

Fig. 1. The coordinate system of the tree trunk.

where V_l is the velocity parallel to the grain, V_r is the velocity perpendicular to the grain (or the velocity along the radial direction), which can be measured by the stress wave testing equipment.

Because $\alpha + \theta = 90°$, formula (1) can be converted into the following forms:

$$V(\theta) = \frac{V_l V_r}{V_l \cos^2 \theta + V_r \sin^2 \theta} \tag{2}$$

or

$$V(\theta)/V_r = \frac{V_l}{V_l \cos^2 \theta + V_r \sin^2 \theta} \tag{3}$$

Let $f(\theta) = V(\theta)/V_r$, and $g(\theta) = V_l \cos^2 \theta + V_r \sin^2 \theta$. From Eq. (3), it can be seen that, if $\theta = 90°$, then $f(\theta) = V_l/V_r$, and that if $\theta = 0°$, then $f(\theta) = 1$.

Now, we approximate Eq. (3) with the second order Taylor polynomial.

The first and second order derivatives of $f(\theta)$ and $g(\theta)$ are calculated as follows.

$$g'(\theta) = -2V_l \cos\theta \sin\theta + 2V_r \sin\theta \cos\theta = -(V_l - V_r)\sin 2\theta \tag{4}$$

$$g''(\theta) = -2(V_l - V_r)\cos 2\theta \tag{5}$$

$$f'(\theta) = -V_l(g(\theta))^{-2} g'(\theta) \tag{6}$$

$$f''(\theta) = -V_l\left(-2(g(\theta))^{-3}(g'(\theta))^2 + (g(\theta))^{-2} g''(\theta)\right) \tag{7}$$

Then

$$g(0) = V_l, \quad g'(0) = 0, \quad g''(0) = -2(V_l - V_r)$$

$$f(0) = 1, \quad f'(0) = 0, \quad f''(0) = -V_l(V_l^{-2}(-2(V_l - V_r))) = \frac{2(V_l - V_r)}{V_l}$$

So, the second order Taylor expansion of $f(\theta)$ at $\theta = 0$ is as follows:

$$f(\theta) = f(0) + \frac{1}{1!}f'(0)\theta + \frac{1}{2!}f''(0)\theta^2 + O(\theta^3)$$

$$= 1 + \frac{V_l - V_r}{V_l}\theta^2 + O(\theta^3) \tag{8}$$

$$\approx 1 + \frac{V_l - V_r}{V_l}\theta^2 \tag{9}$$

In Eq. (8), $O(\theta^3)$ is the remainder of the Taylor polynomial. For the coordinate system given in Fig. 1, we assume the angle $\theta > 0$ if θ is counter-clockwise from the radial direction. Otherwise, $\theta < 0$ if θ is clockwise from the radial direction. Eq. (9) shows that the ratio of $V(\theta)$ to V_r approximates a parabolic curve with the symmetric axis $\theta = 0$, and the second order coefficient $(V_l - V_r)/V_l \in (0, 1)$.

3. Materials and methods

Eight live trees located at the university arboretum in Zhejiang Agricultural and Forestry University were acoustically tested using a ARBOTOM tool (Rinntech, Heidelberg, Germany). The trees tested included Camphor (*Cinnamomum camphora*), Chinese maple (*Acer buergerianum*), abele (*Populus alba*), Chinese catalpa (*Catalpa ovata*) and Chinese red pine (*Pinus tabuliformis*). Fig. 2a shows the field setup of stress wave testing on a camphor tree.

The ARBOTOM unit consisted of twelve impulse sensors with cables, 60 mm sensor pins, and a 12 V rechargeable battery pack. Sensor No. 1 was first attached to the tree trunk through a sensor pin, a meter above the ground. Other eleven sensors were attached to the other side of the trunk and evenly spaced along a vertical